

# A Self Assembled Nanoelectronic Quantum Computer Based on the Rashba Effect in Quantum Dots

S. Bandyopadhyay\*

Department of Electrical Engineering  
University of Nebraska  
Lincoln, Nebraska 68588-0511, USA

## Abstract

Quantum computers promise vastly enhanced computational power and an uncanny ability to solve classically intractable problems. However, few proposals exist for robust, solid state implementation of such computers where the quantum gates are sufficiently miniaturized to have nanometer-scale dimensions. Here I present a new approach whereby a complete computer with nanoscale gates might be self-assembled using chemical synthesis. Specifically, I demonstrate how to self-assemble the fundamental unit of this quantum computer – a 2-qubit universal quantum gate – based on two exchange coupled multilayered quantum dots. Then I show how these gates can be wired using thiolated conjugated molecules as electrical connectors. Each quantum dot in this architecture consists of ferromagnet-semiconductor-ferromagnet layers. The ground state in the semiconductor layer is spin split because of the Rashba interaction and the spin splitting energy can be varied by an external electrostatic potential applied to the dot. A spin polarized electron is injected into each dot from one of the ferromagnetic layers and trapped by Coulomb blockade. Its spin orientation encodes a qubit. Arbitrary qubit rotations are effected by bringing the spin splitting energy in a target quantum dot in resonance with a global ac magnetic field by applying a potential pulse of appropriate amplitude and duration to the dot. The controlled dynamics of the universal 2-qubit rotation operation can be realized by exploiting the exchange coupling with the nearest neighboring dot. The qubit (spin orientation) is read via the current induced between the ferromagnetic layers under an applied potential. The ferromagnetic layers act as “polarizers” and “analyzers” for spin injection and detection. A complete prescription for initialization of the computer and data input/output operations will be presented. This paradigm draws together two great recent scientific advances: one in materials science (nanoscale self assembly) and the other in information science (quantum computing).

---

\*Corresponding author. E-mail: [bandy@quantum1.unl.edu](mailto:bandy@quantum1.unl.edu)

# 1 Introduction

There is significant current interest in quantum computers because they possess vastly enhanced capabilities accruing from quantum parallelism [1, 2]. Some quantum computing algorithms [3, 4] have been shown to be able to solve classically intractable problems. i.e. perform tasks that no classical algorithm could perform efficiently or tractably. Thus, it would be highly desirable to build quantum computers.

Experimental effort in realizing quantum computers has been geared towards synthesizing universal quantum logic gates from which quantum computers can be built. A universal gate is a 2 qubit-gate [5, 6, 7] and has basically two attributes. First, it allows arbitrary unitary rotations on each qubit and second, it performs the quantum controlled rotation operation whereby one of the qubits (the target qubit) is rotated through an arbitrary angle, if, and only if, the other qubit (the control qubit) is oriented in a specified direction. The orientation of the control qubit is left unchanged. It is this conditional dynamics of the controlled rotation operation that is challenging to implement experimentally.

Recently, it has been shown [8, 9, 10] that there exist universal fault-tolerant computers that can operate in a non-ideal noisy environment. They are usually a circuit composed of one- or two-qubit gates performing various unitary rotations on a qubit (e.g Hadamard, Pauli rotations through rational or irrational angles, etc.). They too can in principle be realized that the gate that we discuss here.

The most vexing problem in experimentally realizing quantum computers is the issue of decoherence. Qubits are coherent superpositions of two-level states and as such are delicate entities. Any coupling to the environment will destroy the coherence of the superposition state and corrupt the qubit. Were it not for the recent discovery of quantum error correcting codes [11] that can correct errors due to decoherence through the use of appropriate *software*, quantum computing would have remained a theoretician's pipedream.

In the past, atomic systems were proposed as ideal testbeds for experimental quantum logic gates because of the relatively long coherence times associated with the quantum states of trapped atoms and ions [12]. Experimental demonstrations of quantum logic gates were carried out in atomic systems [13, 14]. Recently, nuclear magnetic resonance (NMR) spectroscopy has been shown to be an attractive alternative [15, 16] and there has been some reports of experimental demonstrations involving NMR [17]. However, there are also some doubts regarding the efficacy of NMR based approaches when dealing with many qubits [18].

The major drawback of both atomic and NMR systems is of course that they are unwieldy, expensive and inconvenient. Solid state (especially nanoelectronic) implementations would be much more desirable because, after all, miniaturization is as important as any other objective and has been fuelling the micro- or nano-electronics revolution for the past four decades. One would like a quantum gate that is one nanometer long and not one meter long. The technology base that exists in the solid-state area with regards to miniaturization is unparalleled.

While it is understood that solid state systems will be preferable vehicles for quantum computation, it is also well-known that the phase memory time of charge carriers in solids

saturate to only a few nanoseconds as the lattice or carrier temperature is lowered to a few millikelvins [19] (this is caused by coupling of carriers to the zero-point motion of phonons). Thus, solid state implementations of quantum gates where the qubits are coupled to charge degrees of freedom will be always dogged by serious decoherence problems. Even though such systems have been proposed in the past [20, 21, 22], they will require clock speeds in the far infra-red frequency range to meet Preskill's criterion for fault-tolerant computing [23].

A possible solution of this problem is to use the spin degrees of freedom in solid state systems to encode qubits since the spin is not coupled to electromagnetic noise and hence should have much longer coherence times than charge. It has been shown that electronic and nuclear spins of phosphorus dopant atoms  $^{31}\text{P}$  in silicon have very long spin-flip times (or the co-called  $T_1$  times in the language of spectroscopy) of about an hour [24]. Consequently, nuclear spins of  $^{31}\text{P}$  dopant atoms in silicon have been advocated as preferable vehicles for qubits [26, 25, 27]. However, the actual coherence time (or  $T_2$  time) of electron spin in P-doped silicon may be on the order of a millisecond. Compound semiconductors may exhibit somewhat shorter spin coherence times, but spin coherence times as long as 100 ns have been experimentally demonstrated in n-type GaAs at the relatively balmy temperature of 5 K [28]. Thus, it is practical to contemplate solid state quantum computers based on single electron spins.

Not all semiconductors however are suitable hosts for qubits. Pyroelectric materials (uniaxial crystals without inversion symmetry) usually exhibit electric dipole spin resonance which can increase the spin flip rate significantly [29] by strongly coupling the spin to phonons. An advantage of quantum dots is that the spin-phonon interaction may be reduced because of a constriction of the phase space for scattering. Moreover, the phonon-bottleneck effect [30] may block phonon-induced spin-flip transitions. Another obvious strategy to increase the coherence time is to decrease the phonon population by reducing the temperature. The temperature must be low in any case since the time to complete a quantum calculation should not significantly exceed the thermal time scale  $\hbar/kT$  [31] irrespective of any other consideration.

Quantum gates based on spin polarized single electrons housed in quantum dots have been proposed by us in the past [32] and more recently by Loss and DiVincenzo [33]. Here we adopt a different idea - which is still based on spin-polarized single electrons - to provide a realistic paradigm for the realization of a *self-assembled* solid-state, nanoelectronic universal quantum gate.

## 2 A Self Assembled Universal Quantum Gate

We will first self assemble a regimented array of *tri-layered* cylindrical quantum dots using an electrochemical technique to be described later. The two outer layers are ferromagnetic and the middle layer is a semiconductor (see Fig. 1).

A dc potential pulse is applied between the two outer (ferromagnetic) layers to inject a

single spin-polarized electron from one of the outer layers into the middle layer. Such spin polarized injection has been demonstrated in the CdMnTe-CdTe system which is shown in Fig. 1(b) [34]. In the middle layer, the electron's ground state is spin-split because of Rashba interaction [35, 36, 37]. The Rashba effect arises from spin-orbit coupling in the presence of a transverse electric field which is always present at the interface of two dissimilar materials owing to the conduction band discontinuity. It is possible to electrostatically *modulate* this spin splitting [39] by applying a potential between the two outer layers. The applied potential alters the interface field that causes the Rashba effect and hence changes the spin-splitting energy. As long as this potential is less than  $e/2C$  ( $e$  is the electron charge and  $C$  is the dot's capacitance) we can change the spin splitting *without* inducing a current flow (causing the injected electron to escape), or causing another electron to be injected. In other words, the electron is trapped in the middle layer of the quantum dot by Coulomb blockade and the applied potential only varies the spin splitting energy.

The trapped electron will couple to both eigenspinors of the dot's ground state [37, 38] unless it was injected with a spin polarization that is an exact eigenspinor. We will show later how to avoid the latter possibility. Thus, the trapped electron will exist in a coherent superposition of the two eigenspinors and form a qubit. Arbitrary qubit (spin) rotations in a selected quantum dot is achieved by bringing its spin-splitting energy in resonance with an external global ac magnetic field by applying the suitable potential between the dot's ferromagnetic outer layers. This allows single qubit rotations.

In order to achieve the conditional dynamics of a universal 2-qubit quantum gate, we need to couple the rotation of one qubit (target qubit) with the orientation of another qubit (control qubit). This can be done via exchange coupling between two single electrons in two neighboring dots. The spin-splitting energy in any dot depends, among other things, on the spin orientation in the neighboring dot if the two dots are exchange coupled. The exchange coupling can be varied by simultaneously applying two independent potentials to the target and control qubits. Thus, the conditional dynamics of the controlled rotation operation can be achieved.

Finally, we have to read a qubit. The qubit (spin orientation in a dot) is read directly via the current induced between the dot's spin polarized outer layers when a sufficiently strong potential is applied to overcome the Coulomb blockade. The magnitude of the current is a measure of the electron's spin polarization. It is possible to read single electron currents using sensitive electrometers.

## 2.1 Rashba effect in a quantum dot

The Hamiltonian for the Rashba interaction is given by

$$H_R = -i [\vec{\sigma} \times \vec{\nabla}] \cdot (\alpha_\nu \hat{\nu}) , \quad (1)$$

where  $\vec{\sigma}$  is the Pauli spin matrix,  $\hat{\nu}$  is the unit vector normal to the interface and  $\alpha_\nu$  is the coupling constant along the  $\nu$ -axis which is proportional to the expected value of the interface electric field along the  $\nu$ -axis [36].

We will use the coordinate system shown in Fig. 1. For mathematical convenience, the quantum dot will be assumed to have a rectangular shape with the dimension along the x-direction much larger than the dimensions along the y- and z-directions. Such a dot is appropriately referred to as a quantum “dash” and is a realistic representation for the type of self-assembly that we will propose.

The Rashba interaction will distort the wavefunction (particle-in-a-box state) of the lowest subband in each dot by causing mixing of the unperturbed subbands. If the dimensions of the quantum dash are small enough that the subbands are well separated in energy, then we can neglect most of the subband mixing and include only the perturbation of the second lowest (or nearest) subband on the lowest subband. This basically requires that the transverse widths of the quantum dash  $W_z$  and  $W_y$  be small enough that they are much smaller than the quantity  $\hbar^2/\alpha m^*$  where  $m^*$  is the electron’s effective mass in the conduction band [37]. In compound semiconductors, the spin-orbit coupling coefficient  $\alpha$  has been experimentally measured and found to be of the order of  $10^{-12}$  eV-m [38]. Hence, we need  $W_z$  and  $W_y$  to be much smaller than about  $0.5 \mu\text{m}$ . In self-assembled structures,  $W_z$  and  $W_y$  are about  $100 \text{ \AA}$  so that we can easily neglect the mixing of transverse subbands (along the y- and z-directions) and include only the effect of the nearest longitudinal subband along the x-direction.

Based on the above consideration, the spatial part of ground state wavefunction of an isolated electron can be written as

$$\psi_{\text{ground}}(\text{spatial}) = \left( \frac{2\sqrt{2}}{W_x W_y W_z} \right) \left( \frac{1}{\sqrt{1 + |a|^2}} \right) \left[ \sin\left(\frac{\pi x}{W_x}\right) + a \sin\left(\frac{2\pi x}{W_x}\right) \right] \sin\left(\frac{\pi y}{W_y}\right) \sin\left(\frac{\pi z}{W_z}\right). \quad (2)$$

The above wavefunction is of course not exact since the electrons are not confined by hardwall boundaries. In fact, hardwall boundaries will not allow the wavefunctions of neighboring electrons to overlap and they need to do so in order to have any residual exchange interaction which is critical to the 2-qubit controlled rotation operation. However, Equation (2) serves as a good zeroth-order estimate for the wavefunction and allows us to evaluate spin eigenstates analytically.

We will assume that  $\alpha_y = \alpha_z = \alpha$  and concentrate on an isolated electron neglecting the exchange interaction between neighbors. Diagonalizing the single-electron Hamiltonian in the basis of Equation (2) yields the eigenenergies of the spin-split ground state:

$$\begin{aligned} E_{\uparrow} &= E_1 + \frac{\sqrt{2}a\alpha p_x}{\hbar} \\ E_{\downarrow} &= E_1 - \frac{\sqrt{2}a\alpha p_x}{\hbar}, \end{aligned} \quad (3)$$

where  $E_1 (= (\hbar^2/2m^*)/[\eta(\pi/W_x)^2 + (\pi/W_y)^2 + (\pi/W_z)^2])$  is the unperturbed ground state energy (lowest subband edge) in the quantum dot,  $\eta = 1 + 3|a|^2/(1 + |a|^2)$ , and  $p_x$  is the momentum matrix element

$$p_x = \langle 1 | -i\hbar \frac{\partial}{\partial x} | 2 \rangle = \frac{8i\hbar}{3W_x}, \quad (4)$$

where  $|1\rangle \equiv \sin\left(\frac{\pi x}{W_x}\right)$  and  $|2\rangle \equiv \sin\left(\frac{2\pi x}{W_x}\right)$ . Since  $p_x$  is purely imaginary, obviously  $a$  is also purely imaginary.

The spin eigenstates associated with lowest spin-split levels (whose eigenenergies are given in Equation (3)) are (in spinor notation)

$$\begin{aligned} |\uparrow\rangle &= \begin{pmatrix} \sqrt{2}+1 \\ i \end{pmatrix} \\ |\downarrow\rangle &= \begin{pmatrix} \sqrt{2}-1 \\ -i \end{pmatrix} \end{aligned} \quad (5)$$

which are orthogonal to each other.

## 2.2 Coherent spin injection from spin polarized contacts

Now assume that the contacts to the quantum dots are single domain Fe-particles which are permanently magnetized along one of the eigenspinor polarizations. It may be possible to obtain almost 100% spin polarization in single domain Fe-alloy particles. Consequently, electrons are almost always injected into one of the spin eigenstates of the semiconductor dot [40]. Injection of spin-polarized electrons into semiconductors have been demonstrated using not Fe-alloy, but dilute semimagnetic semiconductor contacts [34]. Fig 1(b) corresponds to this situation. The disadvantage of CdMnTe (compared to Fe-alloy) is that it is not a permanent magnet and the spin polarization in it needs to be maintained by a globally applied dc magnetic field directed along the  $y$ -direction. However, only a very small field is required since the effective Landé  $g$ -factor for electrons in dilute magnetic semiconductors is huge ( $\sim 100$ ). On the other hand, the advantage of CdMnTe is that it is lattice matched to CdTe and hence interface scattering is less of a problem.

At this juncture, an important question is how easy will it be to maintain single electron occupancy in each dot. As long as the energy cost to add an additional electron ( $= e^2/2C$ ;  $C$  is the capacitance of the dot) significantly exceeds the thermal energy  $kT$ , only a single electron will occupy each dot. Uniform electron occupancy in arrays of  $> 10^8$  dots have been shown experimentally [41].

### 2.2.1 Single qubit rotations

We will now describe how a selected qubit in a quantum dot can be rotated by an arbitrary angle. Note from Equation (3) that the spin-splitting of the ground state depends on the interface spin-orbit coupling coefficient  $\alpha$ . This quantity is proportional to the interface electric field and hence can be modulated by altering the interface potential (in this case the quantum dot's interface with the surrounding insulator ( $\text{Al}_2\text{O}_3$ ) is the relevant interface) by applying an electrostatic field normal to the interface. The applied electric field will also probably alter  $a$  and  $p_x$  thus contributing even more to the modulation of the spin-splitting energy. The possibility of this external electrostatic modulation was predicted by Datta and Das [37] and experimentally demonstrated by Nitta, et. al [39] who were able to vary  $\alpha$

by a factor of 2 by varying the interface potential by 3 V. In self-assembled quantum dots whose geometry is like that in Fig. 1, we will have to apply a potential between the top contact of a dot and the bottom substrate since the sidewalls (interface with  $\text{Al}_2\text{O}_3$ ) are not electrically accessible in this configuration. This is obviously not the best situation because the applied field is primarily parallel to the interface rather than perpendicular. However, there is always a small perpendicular component because of fringing effects and this will alter the spin splitting of the ground state. We can make an estimate of the spin splitting from Equation (3). Assuming that  $|a| = 0.1$ ,  $W_x = 500 \text{ \AA}$  and  $\alpha = 3 \times 10^{-12} \text{ eV-m}$  [38], we find that the spin-splitting energy is  $50 \mu\text{eV}$ . Even a 1% variation of this energy by an applied field would be sufficient. Thus a large applied field is not required.

We cannot apply a large potential over a dot anyway lest we overcome the Coulomb blockade and cause a current to flow between the two spin-polarized contacts. This will collapse the wavefunction by moving the electron inside the contacts which are dissipative. Current flow is allowed only when the qubit has to be read and the information in the read data is discarded thereafter (erasure). Otherwise, we must always operate within the Coulomb blockade regime to avoid dissipation. Assuming that a dot has a capacitance of  $1 \text{ aF}$ , the maximum voltage that we can apply over the dot without breaking the Coulomb blockade and inducing a current flow is  $80 \text{ mV}$ .

In order to rotate the qubit in a selected quantum dot, we will apply a potential pulse of appropriate duration to that dot which will bring the spin splitting energy in that dot in resonance with an applied global ac magnetic field  $B_{ac}$ . This resonance will then rotate the qubit placing it in a coherent superposition of the eigenspinors

$$qubit = a_{\uparrow} | \uparrow \rangle + a_{\downarrow} | \downarrow \rangle . \quad (6)$$

Thus, the desired single qubit rotation can be achieved.

### 2.2.2 2-qubit controlled rotation operation

To perform the operation of the 2-qubit quantum controlled rotation gate, we will require to rotate the spin in the target quantum dot (target qubit) by an arbitrary angle if, and only if, the spin in the neighboring quantum dot (control qubit) is at a specified orientation. The control qubit must remain unchanged in the process. It is obvious that the total spin splitting  $\Delta_{target}$  in the target dot depends, among other things, also on the exchange interaction  $J$  with the neighboring (control) dot (and hence on the spin orientation of the control qubit) if the two dots are exchange coupled. After all, the exchange term will appear in the Hamiltonian of the coupled two-dot system. Thus, the potential  $V_{target}$  that brings the *total* spin splitting energy  $\Delta_{target}$  in the target dot in resonance with the ac magnetic field  $B_{ac}$  depends on the spin orientation in the control dot. Herein lies the possibility of conditional dynamics. We can find the  $V_{target}$  that will rotate the target qubit through an arbitrary angle only if the control qubit is in the specified orientation. Application of this potential  $V_{target}$  to the target dot realizes the operation of a quantum controlled rotation gate.

Alternately, the exchange coupling energy can be varied as well. Since it depends on the tunneling matrix element between neighboring dots and hence on the overlap of their wavefunctions, we can vary it by varying the wavefunctions. This can be applied by applying a differential potential between the two dots which skews the wavefunctions in the dots and changes the overlap. Consequently, once can “tune” the exchange interaction between the electrons in two neighboring dots by independently adjusting the electrostatic potential applied to both of them.

## 2.3 Spin measurement

After quantum computation is over, we need to read the result by measuring the qubits. During this process, the qubits will collapse to classical bits. These classical bits are the measured spin orientations in relevant dots. They are measured by measuring the current that results when the potential over the dot is raised over the Coulomb blockade threshold. If we assume that the differential phase-shift suffered by the spin in traversing the dot is negligible; in other words, transport through the dot does not rotate the spin, then the magnitude of the measured current can tell us the spin orientation [37]. [37]. It was shown in ref. [37] that the spin-polarized contacts act as electronic analogs of optical polarizers and analyzers, so the current will depend on the projection of the spin of the quantum dot’s resident electron on the spin orientation in the contacts. Thus, by measuring the current, we can tell the spin orientation in any quantum dot.

## 2.4 Calibration

For each dot, the potential  $V$  that needs to be applied to flip the spin by bringing the dot in resonance with  $B_{ac}$  can be calibrated following the procedure outlined by Kane [25]. With  $B_{ac} = 0$ , we measure the spin in a quantum dot. Then we switch on  $B_{ac}$  and sweep  $V$  over a range. Next  $B_{ac}$  is switched off and the spin is measured. The range of  $V$  is progressively increased till we find that the spin has flipped. We then proceed to narrow the range with successive iteration while making sure that the spin does flip in each iteration. Finally this allows us to ascertain  $V$  with an arbitrary degree of accuracy. As pointed out by Kane [25], the calibration procedure can, in principle, be carried out in parallel over several dots simultaneously and the voltages stored in adjacent capacitors. External circuitry will thus be needed only to control the timing of the biases (application of  $V_{target}$ ) and not their magnitudes. While this is definitely an advantage, fabricating nanoscale capacitors adjacent to each individual dot is outside the scope of self-assembly. Moreover, capacitors discharge over time, requiring frequent recalibration through refresh cycles, so that this may not be a significant advantage.

## 2.5 Input and Output Operations

Any computer is of course useless unless we are able to input and output data successfully. Since we are using spin-polarized contacts to inject an electron in each dot, we know the initial orientation. Those dots where the initial orientation is the one we want are left unperturbed while the spins in the remaining dots are flipped by resonating with  $B_{ac}$ . This process prepares the quantum computer in the initial state for a computation and can be viewed as the act of “writing” the input data. Computation then proceeds on this initial state by carrying out a desired sequence of controlled rotation operations. Reading the data is achieved as described in subsection 2.3.

## 3 Self Assembly

We now describe how the quantum computer is self-assembled. The self-assembly process is relatively standard and has been successfully applied by a number of groups, including us, for fabricating ordered two-dimensional arrays of quantum dots or nanowires [42]. The synthesis proceeds as follows.

First an Al foil is dc anodized in 15% sulfuric acid for several hours with a current density of 40 mA/cm<sup>2</sup>. This produces a nanoporous alumina film on the surface of the foil with a quasi-ordered arrangement of pores. The film is stripped off and the foil is re-anodized for a few minutes. The alumina film that forms on the surface after the second anodization step has a very well ordered arrangement of nanopores [43]. Fig. 2 shows a raw atomic force micrograph of pores formed by anodizing in oxalic acid. The pore diameter is 52 nm and the thickness of the wall separating two adjacent pores is of the same order. If the anodization is carried out in sulfuric acid, the pores that self-assemble have a much smaller diameter of  $10 \pm 1$  nm with a wall thickness of the same order [42]. Cross-section TEM of the pores have revealed that they are cylindrical with very uniform diameter along the length. The length of the pores is of course the thickness of the alumina film and depends on the duration of anodization. Typically, the length is a few thousands of angstroms.

Multilayered quantum dots as shown in Fig. 1 are formed by sequentially electrodepositing the constituent layers selectively within the pores. However, in order to have appreciable overlap of the wavefunctions in neighboring dots for exchange coupling, we must first decrease the thickness of the alumina walls separating two adjacent dots. The separation can be decreased to as small as  $\sim 1$  nm by widening the pores. This is accomplished by soaking the porous alumina film in phosphoric acid which dissolves the alumina from the walls of the pores. We have indirect experimental evidence that this indeed increases the exchange coupling between neighboring dots [44].

Electrodeposition of the constituent layers of a multi-layered quantum dot (or quantum dash) is carried out in steps. For depositing the first Fe layer, the alumina film is immersed in a solution of  $\text{FeSO}_4$  and an ac signal of 20 V rms amplitude and 250 Hz frequency is imposed between the aluminum substrate and a graphite counter electrode. During the cathodic half cycle of the ac signal, the  $\text{Fe}^{++}$  ion is reduced to zero-valent Fe metal which

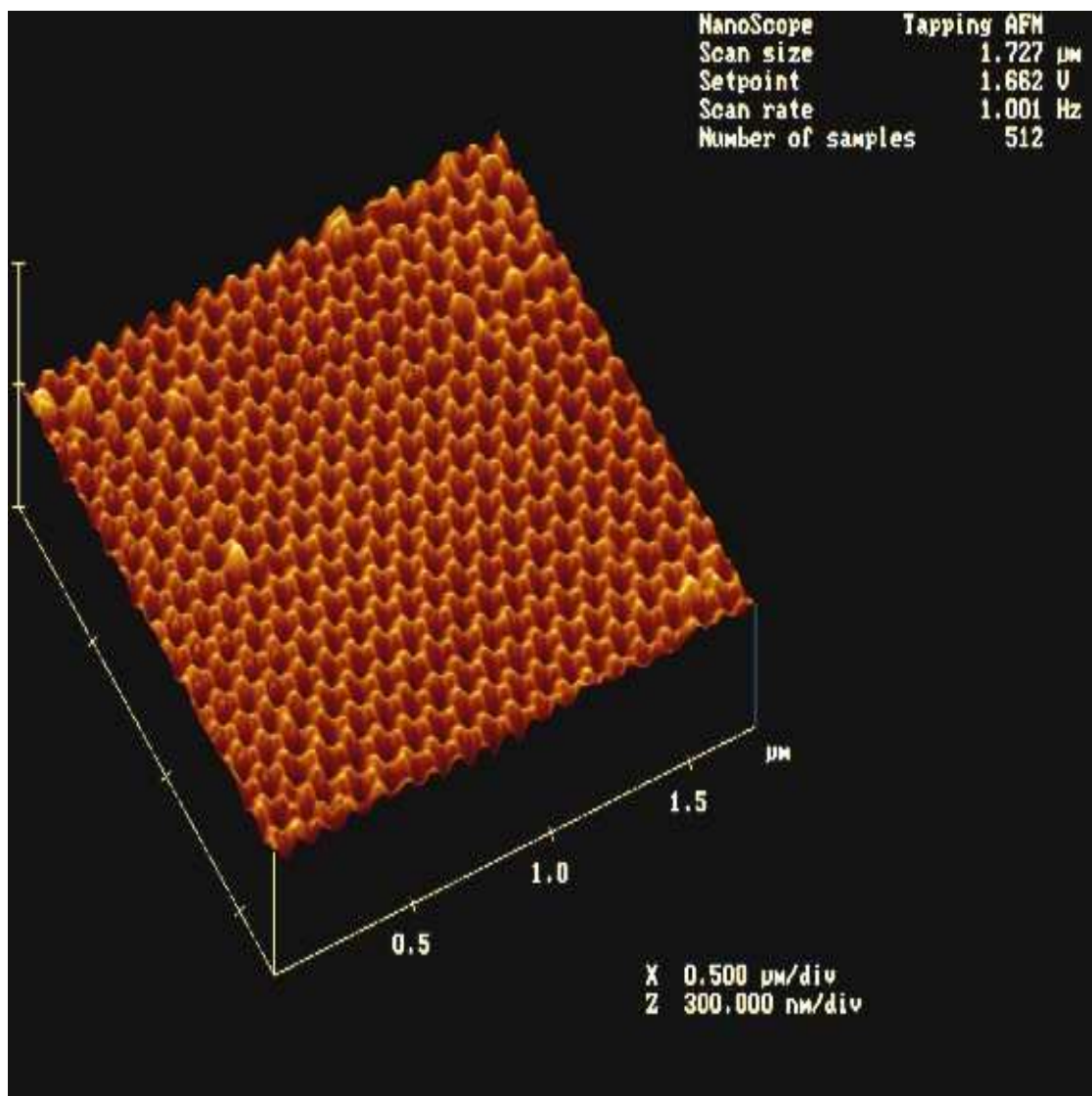


Figure 1: Atomic force micrograph of pore morphologies produced by anodization of an aluminum foil in oxalic acid. The average pore diameter is 52 nm with a 5% standard deviation.

goes into pores selectively since they offer the least impedance path for the ac current to flow. Since alumina is a valve metal oxide, the zero-valent Fe is not re-oxidized to  $\text{Fe}^{++}$  during the anodic half-cycle. After a few seconds of electrodeposition, we are left with a  $\sim$  10-nm layer of Fe at the bottom of the pore.

The partially filled alumina film is then ac electrolysed in sulfuric acid for a few seconds which leaves behind the  $\text{S}^{--}$  ions adsorbed on the walls of the pores. Next, the sample is immersed in a boiling solution of  $\text{CdSO}_4$ . The  $\text{Cd}^{++}$  ion reacts with the  $\text{S}^{--}$  in the walls of the pore to produce a  $\sim$  10-nm thick layer of  $\text{CdS}$  on top of the Fe layer. Finally, another  $\sim$  10-nm thick layer of Fe is deposited on top. This results in the structure of Fig. 1(a). Note that the spin-polarized contacts are automatically *self-aligned* to the semiconductor dot in this approach.

If we wish to self-assemble the alternate structure in Fig. 1(b), we will use telluric acid instead of sulfuric acid for the ac electrolysis.  $\text{CdMnTe}$  is deposited by immersing the alumina film in a boiling solution of  $\text{CdSO}_4$  and  $\text{MnSO}_4$ , whereas  $\text{CdTe}$  is deposited by immersing in a solution of pure  $\text{CdSO}_4$ .

Material purity is of extreme concern in any electrochemical synthesis. Chemical reagents are never very pure and we certainly do not want a magnetic impurity in the semiconductor dot that will tend to cause unwanted spin flips. It is possible to fill the pores using very slow deposition in an MBE set-up. This will guarantee vastly improved material purity with a commensurate increase in cost.

### 3.1 Wiring the gates to make a computer

Arbitrary connections will have to be made between different gates in order to make a computer. The lithographic challenge associated with this task is daunting; however, there is an alternate. We can deposit Au over the top Fe-alloy contact in the same way as we deposit Fe-alloy. Gold sulfide is an appropriate electrochemical source for gold. Conjugated organic molecules such as biphenyl dithiol and gold clusters can be co-evaporated on the surface after each pore is sealed with a top Au layer. The end-group in the organic molecule self-attaches to Au acting as “alligator-clips” [45, 46]. The molecules bridged by Au clusters (Fig. 3) are electrically conducting with a resistance of 10-40  $\text{M}\Omega$  per molecule [47, 48]. They are called “molecular ribbons” and provide *self-assembled* electrical connection between the quantum dots (Fig. 3). However, the connection exists between every dot and hence must be surgically modified to realize a specific interconnection pattern. For this purpose, one will need to remove the unwanted connections with an STM tip. This is a slow and laborious process but still beats lithography.

Lithography however is not completely unavoidable. Connections to the external world for data input/output to the entire chip must be delineated with lithography. This is however not as demanding as making all the internal connections (dot-to-dot connections) with lithography.

## 4 Conclusions

In this paper, we foresee the application of a great advance in materials technology, nanoscale self-assembly, to realize a great advance in information technology - the quantum computer. In the past, semiconductor implementations of quantum computers were proposed with nuclear spins of donor atoms in silicon used as qubits [25] and rotations being performed using hyperfine interactions. Such proposals require extremely challenging fabrication methodologies and rely on delicate interaction between nuclear and electron spins to transduce the qubit into a measurable signal. The present paradigm is much simpler, probably more robust, and the possibility of self-assembly makes it very attractive.

## References

- [1] B. Schumacher, *Phys. Rev. A*, **51**, 2738-2747 (1995).
- [2] A. Steane, *Rep. Prog. Phys.*, **61**, 117-173 (1998).
- [3] P. W. Shor, in *Proc. 35th. Ann. Symp. Foundations of Computer Science*, Ed. S. Goldwasser, pp. 124-134 (IEEE Computer Society, Los Alamitos, CA, 1994).
- [4] L. K. Grover, *Phys. Rev. Lett.*, **79**, 325-328 (1997); L. K. Grover, *Phys. Rev. Lett.*, **79**, 4709-4712 (1997).
- [5] D. P. DiVincenzo, *Phys. Rev. A*, **51**, 1015-1021 (1995).
- [6] S. Lloyd, *Phys. Rev. Lett.*, **75**, 346-349 (1995).
- [7] A. Barenco, *Proc. R. Soc. London*, **A449**, 679-683 (1995).
- [8] P. W. Shor in *Proc. 37th Ann. Symp. Foundations of Comp. Sci.*, IEEE Computer Society Press, pp. 56-65 (1996).
- [9] A. Kitaev, *Russian Math Surveys*, **52**, 1191 (1997).
- [10] P. O. Boykin, T. Mor, M. Pulver, V. Roychowdhury and F. Vatan, LANL e-print quant-ph #9906054.
- [11] A. R. Calderbank and P. W. Shor, *Phys. Rev. A*, **54**, 1098-1105 (1996).
- [12] J. I. Cirac and P. Zoller, *Phys. Rev. Lett.*, **74**, 4091-4094 (1995).
- [13] Q. A. Turchette, C. J. Hood, W. Lange, H. Mabuchi and H. J. Kimble, *Phys. Rev. Lett.*, **75**, 4710-4713 (1995).
- [14] C. Monroe, D. M. Meekhof, B. E. King, W. M. Itano and D. J. Wineland, *Phys. Rev. Lett.*, **75**, 4714-4717 (1995).
- [15] D. G. Cory, A. F. Fahmy T. F. and Havel, in *Proc. 4th Workshp. on Physics and Computation*, (Complex Systems Institute, Boston, MA, 1996). See also, D. G. Cory, M. G. Price and T. F. Havel, *Proc. Natl. Acad. Sci., USA*, **94**, 1634-1639 (1997).
- [16] N. A. Gershenfeld and I. L. Chuang, *Science*, **275**, 350-356 (1997).
- [17] J. A. Jones and M. Mosca, *Phys. Rev. Lett.*, **83**, 1050-1053 (1999).
- [18] S. L. Braunstein, C. M. Caves, R. Josza, N. Linden, S. Popescu and R. Schack, *Phys. Rev. Lett.*, **83**, 1054-1057 (1999).
- [19] P. Mohanty, E. M. Q. Jariwalla and R. A. Webb, *Phys. Rev. Lett.*, **78**, 3366-3369 (1997).

- [20] A. Barenco, D. Deutsch and A. Ekert, *Phys. Rev. Lett.*, **74**, 4083-4087 (1995).
- [21] S. Bandyopadhyay, A. Balandin, V. P. Roychowdhury and F. Vatan, *Superlat. Microstruct.*, **23**, 445-464 (1998).
- [22] A. Balandin and K. L. Wang, *Superlat. Microstruct.*, **25**, 509 (1999).
- [23] J. Preskill, *Proc. Royal Soc. London A*, **454**, 385 (1998).
- [24] G. Feher, *Phys. Rev.*, **114**, 1219 (1959).
- [25] B. E. Kane, *Nature* (London), **393**, 133-137 (1998).
- [26] V. Privman, I. D. Vagner and G. Kvetsel, *Phys. Lett. A*, **239**, 141 (1998).
- [27] R. Vrijen, E. Yablonovitch, K. Wang. H. W. Jianh, A. Balandin, V. Roychowdhury, T. Mor and D. DiVincenzo, LANL e-print quant-ph #9903042.
- [28] J. M. Kikkawa and D. D. Awschalom, *Phys. Rev. Lett.*, **80**, 4313 (1998).
- [29] R. Romestain, S. Geschwind and G. E. Devlin, *Phys. Rev. Lett.*, **39**, 1583 (1977).
- [30] H. Benisty, C. M. Sotomayor-Torres and C. Weisbuch, *Phys. Rev. B*, **44**, 10945 (1991).
- [31] W. G. Unruh, *Phys. Rev. A*, **51**, 992 (1995).
- [32] S. Bandyopadhyay and V. P. Roychowdhury, *Superlat. Microstruct.*, **22**, 411 (1997).
- [33] D. Loss and D. P. DiVincenzo, *Phys. Rev. A*, **57**, 120 (1998).
- [34] M. Oestreich, J. Hübner, D. Hägele, P. J. Klar, W. Heimbrodt, W. W. Rühle, D. E. Ashenford and B. Lunn, *Appl. Phys. Lett.*, **74**, 1251-1253 (1999).
- [35] E. I. Rashba, *Sov. Phys. Semicond.*, **2**, 1109-1122 (1960); Y. A. Bychkov and E. I. Rashba, *J. Phys. C*, **17**, 6039-6045 (1984).
- [36] G. Lommer, F. Malcher, and U. Rössler, *Phys. Rev. Lett.*, **60**, 728-731 (1988).
- [37] S. Datta and B. Das, *Appl. Phys. Lett.*, **56**, 665-667 (1990).
- [38] B. Das, D. C. Miller and S. Datta, *Phys. Rev. B*, **39**, 1411 (1989).
- [39] J. Nitta, T. Akazaki, H. Takayanagi, and T. Enoki, *Phys. Rev. Lett.* **78**, 1335-1339 (1997).
- [40] M. Johnson and R. H. Silsbee, *Phys. Rev. B*, **37**, 5312 (1988).
- [41] B. Muerer, D. Heitman and K. Ploog, *Phys. Rev. Lett.*, **68**, 1371 (1988).

- [42] See, for example, S. Bandyopadhyay, A. E. Miller, H-C Chang, G. Banerjee, V. Yuzhakov, D-F Yue, R. E. Ricker, S. Jones, J. A. Eastman, E. Baugher and M. Chandrasekhar, *Nanotechnology*, **7**, 360-371 (1996) and references therein.
- [43] H. Masuda and M. Satoh, *Jpn. J. Appl. Phys.*, **35**, L126 (1996).
- [44] L. Menon, M. Zheng, H. Zeng, Sellmyer and S. Bandyopadhyay, in *Advanced Luminescent Materials and Quantum Confinement*, Eds. M. Cahay, S. Bandyopadhyay, D. J. Lockwood, N. Koshida, J-P Leburton, M. Meyyappan and T. Sakamoto (The Electrochemical Society, Inc., Pennington, New Jersey, 1999), pp. 413-424.
- [45] J. M. Tour and J. S. Schumm, *Polym. Prepr.*, **34**, 368 (1993).
- [46] J. I. Henderson, S. Feng, G. M. Ferrence, T. Bein and C. P. Kubiak, *Inorg. Chim. Acta*, **242**, 115 (1996).
- [47] R. P. Andres, T. Bein, M. Dorogi, S. Feng, J. I. Henderson, C. P. Kubiak, W. J. Mahoney, R. G. Osifchin and R. Reifenberger, *Science*, **272**, 1323 (1996).
- [48] R. P. Andres, J. D. Bielefeld, J. I. Henderson, D. B. Janes, V. R. Kolagunta, C. P. Kubiak, W. J. Mahoney and R. G. Osifchin, *Science*, **273**, 1690 (1996).

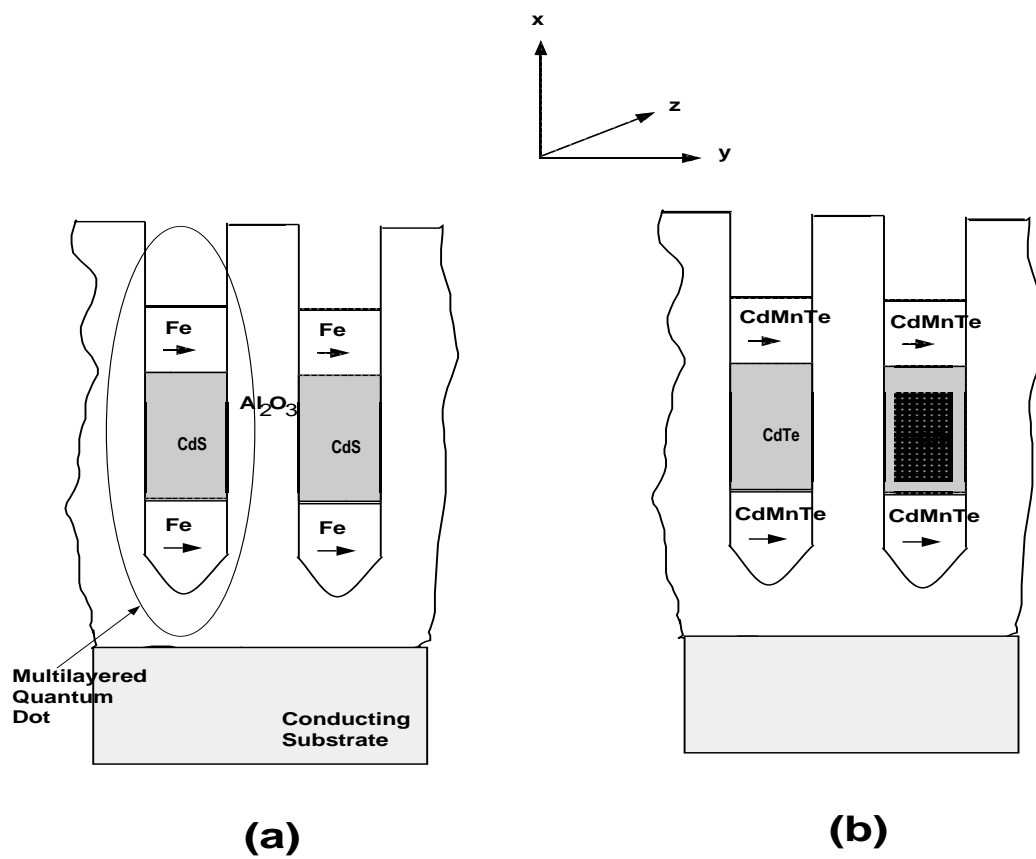


Figure 2: Two multilayered quantum dots (or quantum dashes) separated by an insulating barrier. Each dot or dash consists of a semiconductor sandwiched between two self-aligned spin polarized contacts. (a) Fe-CdS-Fe and (b) CdMnTe-CdTe-CdMnTe.

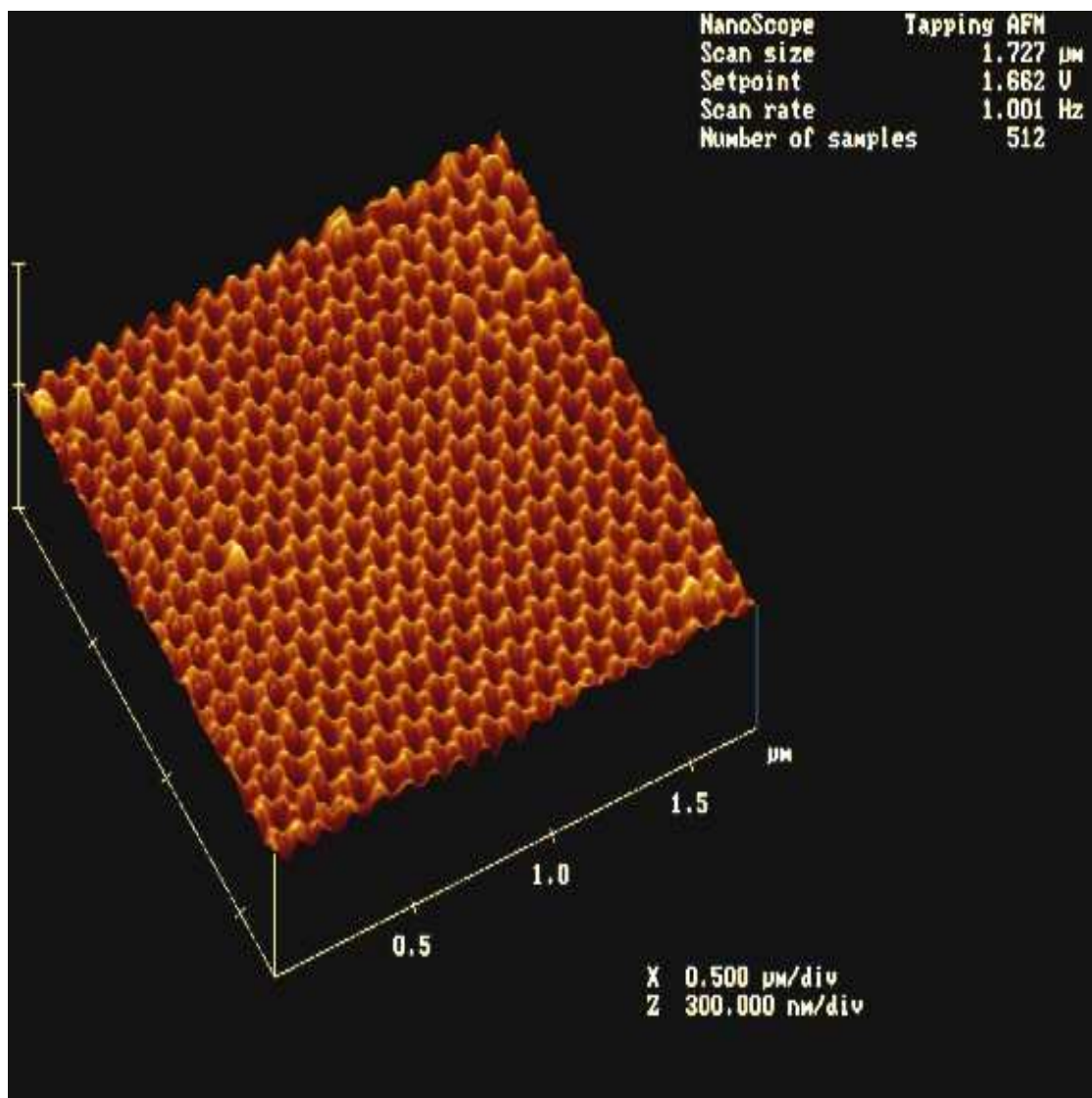


Figure 3: Atomic force micrograph of pore morphologies produced by anodization of an aluminum foil in oxalic acid. The average pore diameter is 52 nm with a 5% standard deviation.

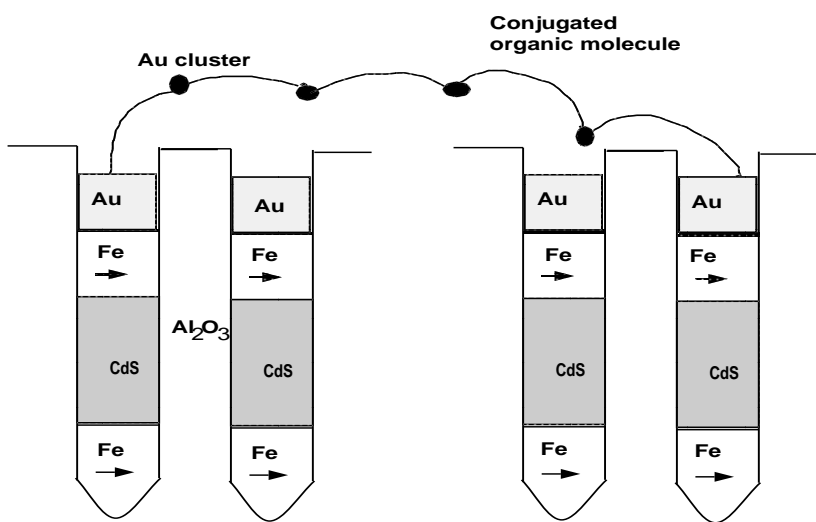


Figure 4: Wiring the quantum computer. Dot-to-dot connections are self-assembled using conjugated organic molecules with appropriate end-groups that self-adhere to gold. Gold clusters act as links in the bridge. Every Au contact is connected to others via the linked molecules and the unwanted connections are subsequently removed with an STM tip.